Mine Water and the Environment (2019) 38:335–341
https://doi.org/10.1007/s10230-018-0561-x

TECHNICAL ARTICLE

Exfoliated Graphitic Carbon Nitride for the Fast Adsorption of Metal Ions from Acid Mine Drainage: A Case Study from the Sungun Copper Mine

Afshin Akbari Dehkharghani[1]

Received: 10 October 2017 / Accepted: 10 September 2018 / Published online: 19 September 2018

Abstract
Graphitic carbon nitride (g-C_3N_4) was easily synthesized from melamine and subsequently sonicated to create exfoliated g-C_3N_4. Samples were characterized with scanning electron and transmission electron microscopy, X-ray diffraction, N_2 adsorption–desorption, and Fourier transformed infrared analysis. The un-exfoliated and exfoliated g-C_3N_4 were both assessed as adsorbents for the removal of Cu^{2+}, Mn^{2+}, Zn^{2+}, Pb^{2+}, Fe^{3+}, and Cd^{2+} from synthetic solutions and acid mine drainage (AMD) from the Sungun copper mine in Iran. Batch adsorption experiments were conducted to evaluate the adsorption process. The results indicated that the sorption capacities of the g-C_3N_4 remarkably increased after sonication, apparently indicating that the sorption mechanisms were largely due to chemical interactions between the metal ions and functional groups on the g-C_3N_4 surface. The kinetic study clarified that the adsorption process followed a pseudo-second-order kinetic model. The sorption isotherms of all of the metal ions on the exfoliated g-C_3N_4 correlated well with both Langmuir and Freundlich adsorption isotherms. Sorption experiments using both the AMD and the multi-component solutions clarified that exfoliated g-C_3N_4 has good potential for AMD treatment.

Keywords g-C_3N_4 · Sonication treatment · Adsorption process · Iran

Introduction

Removal of metal ions from industrial wastewater has aroused global attention due to their adverse effect on the environment and human health. The pollution of water resources by the indiscriminate disposal of metals has been causing escalating worldwide concerns over three centuries of industrialization (Fu and Wang 2011; Rahimi and Mohaghegh 2016; Ren et al. 2011; Srivastava and Majumder 2008). Acid mine drainage (AMD) and the metal ions from mine waste and tailings leachates must be treated before its release to prevent contamination of the food chain (Akcil and Koldas 2006; Skousen et al. 2017).

Many methods, including chemical precipitation (Fu and Wang 2011; Huisman et al. 2006), sorption (Rahimi and Mohaghegh 2016), reverse osmosis (Ning 2002), and ion exchange (Cheng et al. 2010) have been proposed to eliminate metal ions from water resources. Of these, adsorption is quite interesting because of its low costs, ease of operation, and wide adaptability. So far, several types of adsorbents, including carbon nanotube-based composites (Wang et al. 2013), activated carbon (Alslaibi et al. 2013), metal organic framework (Rahimi and Mohaghegh 2017), zeolites (Motsi et al. 2009), biomaterials (Minamisawa et al. 2004), and graphene (Zhao et al. 2011) have been investigated. However, the difficult procedures to synthesize these materials and modify them have limited their commercial uses. Therefore, easily synthesized, efficient adsorbent materials are still needed.

Carbon nitride is a metal-free material that has various potential applications (Goettmann et al. 2006a, b). Based on theoretical calculations, there are five crystalline structures of carbon nitride, of which "g-C_3N_4" is the most stable allotrope of carbon nitride at ambient conditions (Hu et al. 2015;

Electronic supplementary material The online version of this article (https://doi.org/10.1007/s10230-018-0561-x) contains supplementary material, which is available to authorized users.

✉ Afshin Akbari Dehkharghani
a.akbari_dekhovarghani@iauctb.ac.ir

[1] Department of Petroleum, Mining and Material Engineering, Islamic Azad University, Central Tehran Branch, Tehran, Iran

Shen et al. 2015). The $–NH_2$/–NH–/=N functional groups of g-C_3N_4 can adsorb organic and inorganic molecules, including metal ions (Hu et al. 2015; Shen et al. 2015; Yan et al. 2013). However, to the best of our knowledge, its potential use to adsorb metal ions from AMD has not been studied.

The sorption characteristics and uptake efficiency of Cu^{2+}, Fe^{3+}, Mn^{2+}, Zn^{2+}, Cd^{2+}, and Pb^{2+} ions from aqueous solutions similar to AMD from the Sungun copper mine using un-exfoliated and exfoliated g-C_3N_4 nano-adsorbents were therefore studied. The g-C_3N_4 nano-adsorbents were characterized by several techniques and the mechanism of metal ion sorption, sorption kinetics, and isotherms were investigated. Experiments to determine how well the g-C_3N_4 nano-adsorbents worked were performed using actual AMD from the Sungun mine.

Experimental

Materials

AMD wastewater from the Sungun mine was used to study the sorption activity of the un-exfoliated and exfoliated g-C_3N_4 adsorbents. All of the materials used for adsorbent fabrication were used without further purification.

Apparatus

The X-ray diffraction (XRD) patterns were produced on a Philips X'pert instrument using Cu Kα irradiation (λ = 0.15406 nm) as the X-ray source. Morphological characteristics were analysed by field emission scanning electron microscopy (FE-SEM, XL30 model) and transmission electron microscopy (TEM). Fourier transformed infrared (FT-IR) spectra were used to investigate the surface functional groups of the g-C_3N_4 adsorbents. The specific surface area and pore volume distributions of the adsorbents were obtained at 77 K, based on the nitrogen adsorption–desorption isotherms. The metal ion concentrations in each sorption test were determined using a Shimadzu 6300 atomic absorption spectrophotometer (AAS).

Fabrication of Un-exfoliated and Exfoliated g-C_3N_4

Un-exfoliated g-C_3N_4 powders were fabricated by calcining melamine, as previously reported (Li et al. 2013). The melamine (6 g) was placed in a semi-closed crucible at 500 °C in a muffle furnace (with a heating rate of 10 °C/min). The crucible was maintained at this temperature for 4 h and then it was heated to 520 °C at the same rate for 2 h. To exfoliate the g-C_3N_4, the g-C_3N_4 powder was dispersed in 30 mL of deionized water by sonication for 3 h and then magnetically stirred for 24 h. The resulting light-yellow products were centrifuged to remove the residual un-exfoliated g-C_3N_4.

Sorption Batch Experiments

For the sorption tests, a circulating water jacket was placed on the batch reactor to maintain a constant temperature. The reactor was first filled with 200 mL of a synthesized solution, that included metal ions (Cu^{+2}, Mn^{+2}, Cd^{+2}, Zn^{+2}, Fe^{+3}, and Pb^{+2} at concentrations of 228.1, 112.4, 35.9, 91.7, 73.7, and 35.1 mg/L, respectively) and then 0.1 g of one of the adsorbents was fed into the reactor with stirring. At timed intervals, 4 mL of solution was taken out, centrifuged, and submitted for AAS analysis. By performing a proper material balance, the quantity of ions adsorbed was determined at regular time intervals.

For the AMD treatment, 1000 mL of AMD and 0.1 g of the adsorbents were fed into the described reactor. The Cu^{+2}, Mn^{+2}, Cd^{+2}, Zn^{+2}, Fe^{+3} and Pb^{+2} concentrations in the Sungun AMD sample were 228.1, 112.4, 35.9, 91.7, 73.7, and 35.1 mg/L, respectively.

Results and Discussion

XRD Analysis

The graphitic stacking structure of both the un-exfoliated and exfoliated g-C_3N_4 was investigated by XRD (Fig. 1). In the case of the un-exfoliated g-C_3N_4, sharp and strong diffraction peak at 28.1° corresponding to the (002) plan can be ascribed to the stacking of the conjugated aromatic system

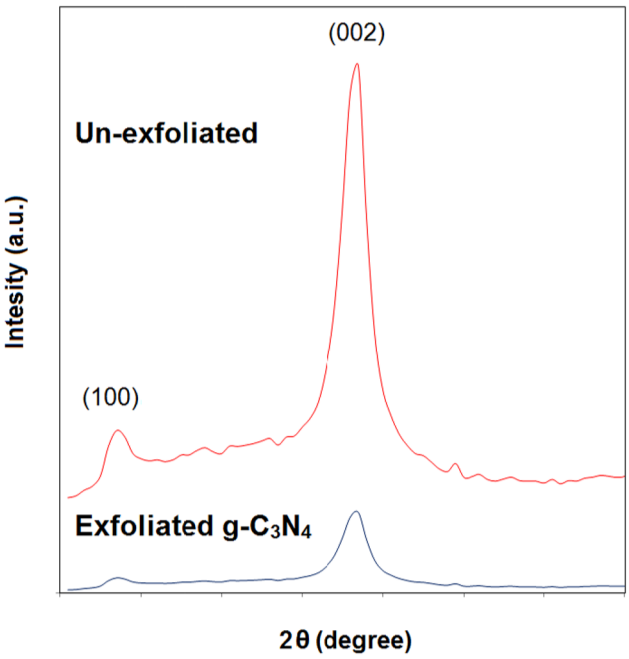

Fig. 1 XRD pattern of the both un-exfoliated and exfoliated g-C_3N_4

with a d-spacing of 0.317 nm. The peak around 13.02° is related to the in-planar repeating motifs of a continuous heptazine network with a d-value of 0.681 nm in g-C_3N_4 crystal (Hu et al. 2015; Shen et al. 2015). After exfoliation via sonication, the intensity of the (002) peak greatly decreases, obviously showing that un-exfoliated g-C_3N_4 has been successfully exfoliated.

FT-IR Spectroscopy

The FT-IR spectrum of exfoliated g-C_3N_4 adsorbent is represented in Fig. 2a. The main absorption band at about 1409, 1462, 1573, and 1640 cm^{-1} are assigned to the stretching vibration modes of heptazine-derived rings (Fig. 2b). Peaks at 1240 and 1320 cm^{-1} correspond to the secondary and tertiary (C–N) amine fragments, respectively. In addition, the wide band at 3200 cm^{-1} belongs to the stretching vibration of $–NH_2–$ and –NH– (Hong et al. 2016; Li et al. 2017). The residual H atoms bind to the edges of the g-C_3N_4 sheets as $C–NH_2$ and 2C–NH bonds. The band at 811 cm^{-1} belongs to the breathing mode of s-triazin (Fig. 2b; Hu et al. 2015). As a reference, the FTIR spectrum of un-exfoliated g-C_3N_4 was also evaluated, but is not shown here. Obviously, the spectrum of the un-exfoliated g-C_3N_4 is similar to that of exfoliated g-C_3N_4, demonstrating that the exfoliated nanosheets keep the same chemical structure as the un-exfoliated one.

SEM and TEM Analysis

The morphologies of the un-exfoliated g-C3N4 sample were investigated by SEM and overlapping lamellar structures were observed (Supplemental Fig. S-1). However, TEM showed the completely lamellar morphologies of the exfoliated g-C3N4 (Supplemental Fig. S-2), demonstrating that the exfoliation of bulk g-C3N4 was successful. These results are consistent with the XRD results.

BET Surface Area Analysis

Table 1 shows the specific surface area and total pore volume information for un-exfoliated and exfoliated g-C_3N_4 nano-adsorbents. High specific surface area is generally needed

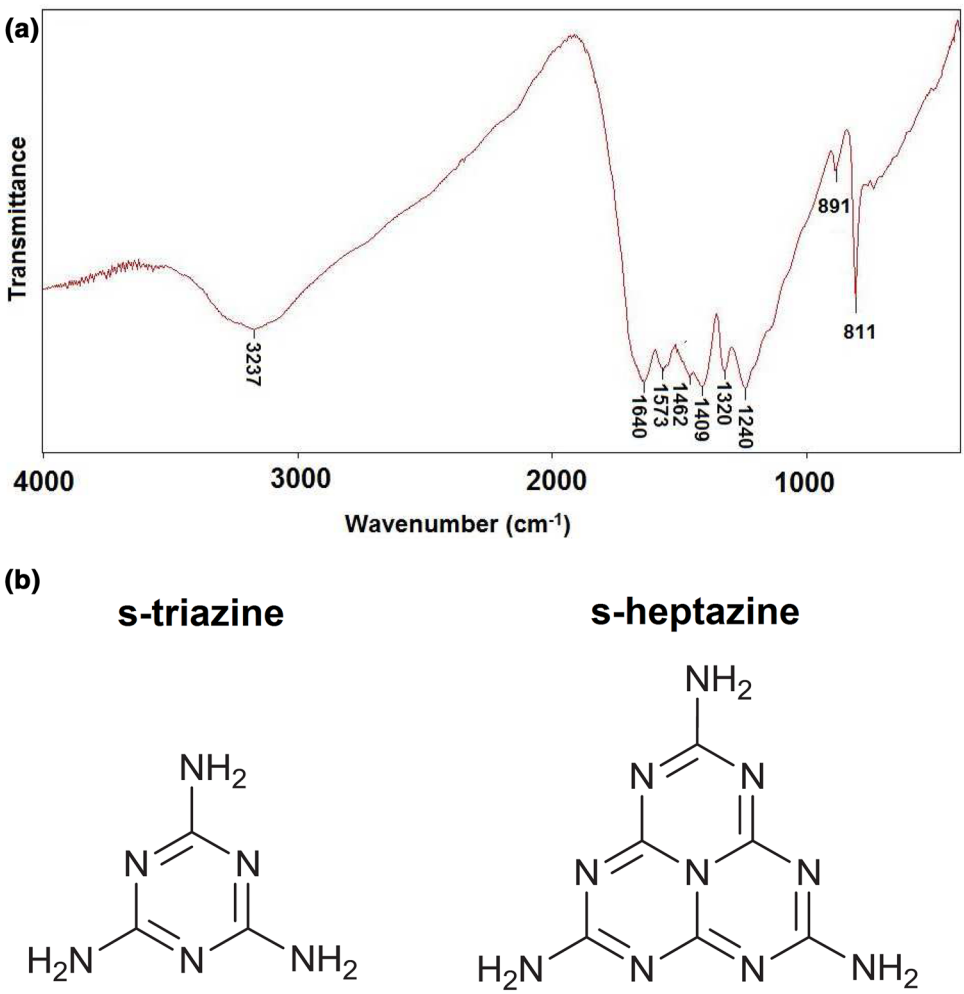

Fig. 2 **a** FT-IR spectrum of the g-C_3N_4 adsorbent and **b** s-heptazine unit and s-triazine unit structures

Table 1 Properties of the adsorbents

Adsorbents	S_{BET} ($m^2\ g^{-1}$)	Total pore volume ($cm^3\ g^{-1}$)
Un-exfoliated g-C_3N_4	196.0	0.38
Exfoliated g-C_3N_4	243.2	0.80

to promote the adsorption of metal ions. As seen in Table 1, exfoliated g-C_3N_4 has a higher surface area than the un-exfoliated g-C_3N_4.

Sorption Study

The sorption of metal ions on the un-exfoliated and exfoliated g-C_3N_4 adsorbents were studied (Fig. 3). The metal ion uptake was higher with the exfoliated g-C_3N_4 adsorbents than the un-exfoliated ones, indicating that sonication improved the adsorption, presumably by increasing the surface area, although reactive amino groups on the surface of exfoliated g-C_3N_4 probably also contribute to the high metal ion removals. Additionally, as seen in Fig. 3, sorption efficiency increases quickly at the first contact time. This fast sorption of the metal ions demonstrates that surface complexation or chemical reaction is taking place (Hu et al. 2015; Shen et al. 2015), along with interaction of the metal ions with the nitrogen- and carbon-containing functional groups of the g-C_3N_4. Thus, inner-sphere surface complexation suitably explains this fast sorption. The total removal processes of metal ions with the exfoliated g-C_3N_4 are schematically represented in Fig. 4.

Kinetics Studies

To better evaluate the sorption mechanism, the experimental data were fit to a pseudo-second-order rate model (Eq. 1). A pseudo-second-order rate model is consistent with the assumption that the determining rate step may be chemical sorption (valence forces formed by electronic interaction between the adsorbents and adsorbates) (Hu et al. 2015; Rahimi and Mohaghegh 2016; Shen et al. 2015).

$$\frac{dq_t}{dt} = k(q_e - q_t)^2 \quad (1)$$

Separating the variables in Eq. 1 yields:

$$\frac{dq_t}{(q_e - q_t)^2} = kdt \quad (2)$$

where q_e is the amount of adsorbed per unit mass at equilibrium, q_t is the amount of metal ions adsorbed at time t (mg g^{-1} adsorbent) and k is the second order rate constant

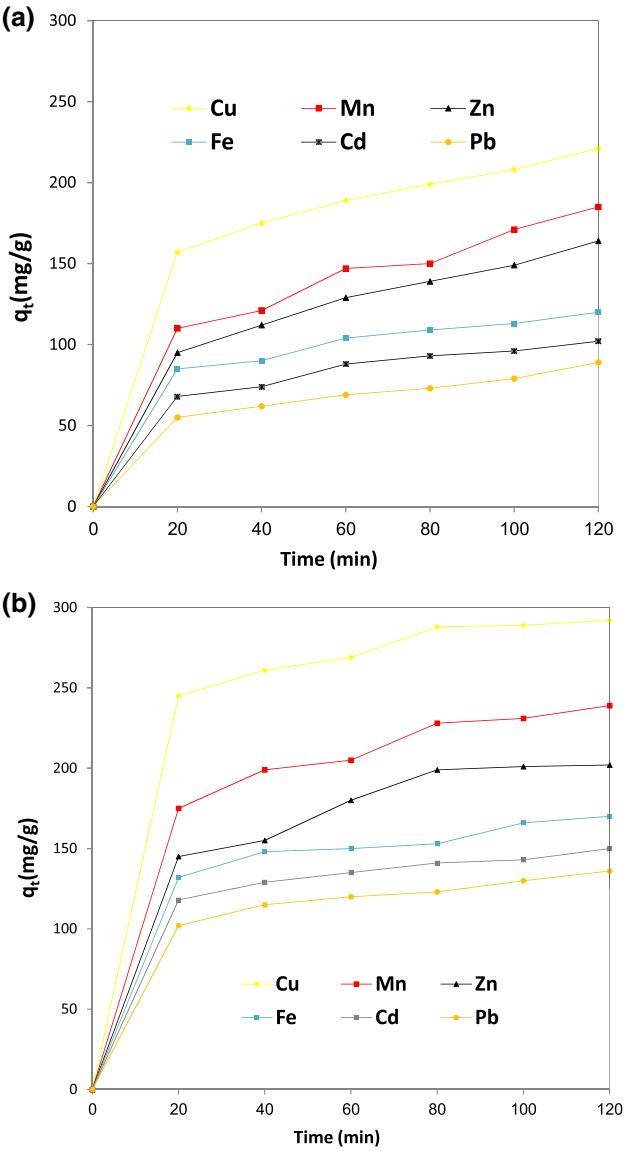

Fig. 3 Removal efficiency of metal ions from synthetic solution with **a** un-exfoliated and **b** exfoliated g-C_3N_4 (pH 7, Contact time = 120 min, T = 25 °C)

(g mg^{-1} min^{-1}). A linear form of the typical second-order rate equation is represented by Eq. 3, in which x can be evaluated from Eq. 4:

$$\frac{t}{q_t} = \frac{1}{x} + \frac{1}{q_e}t \quad (3)$$

$$x = kq_e^2 \quad (4)$$

The pseudo-second-order model constants can be calculated from the linear plots of $\frac{t}{q_t}$ versus time t (Fig. 5).

The aforementioned equations account for the wide range of results and can be used to analyse the isotherm data. The

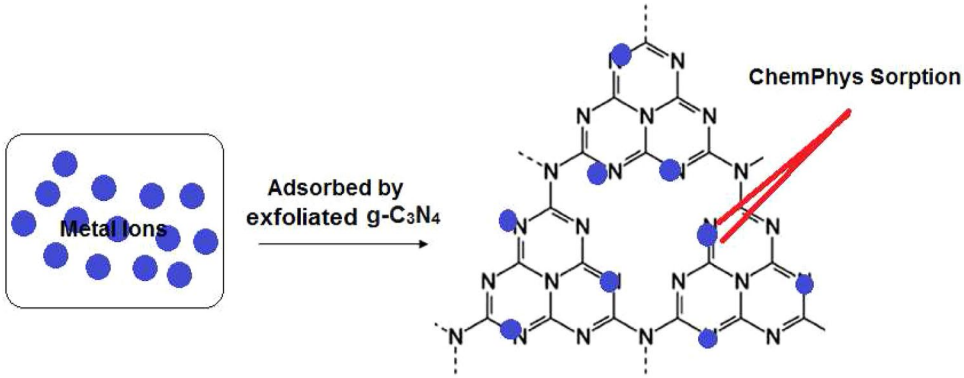

Fig. 4 Total removal processes of metal ions with exfoliated g-C_3N_4 nanoadsorbents

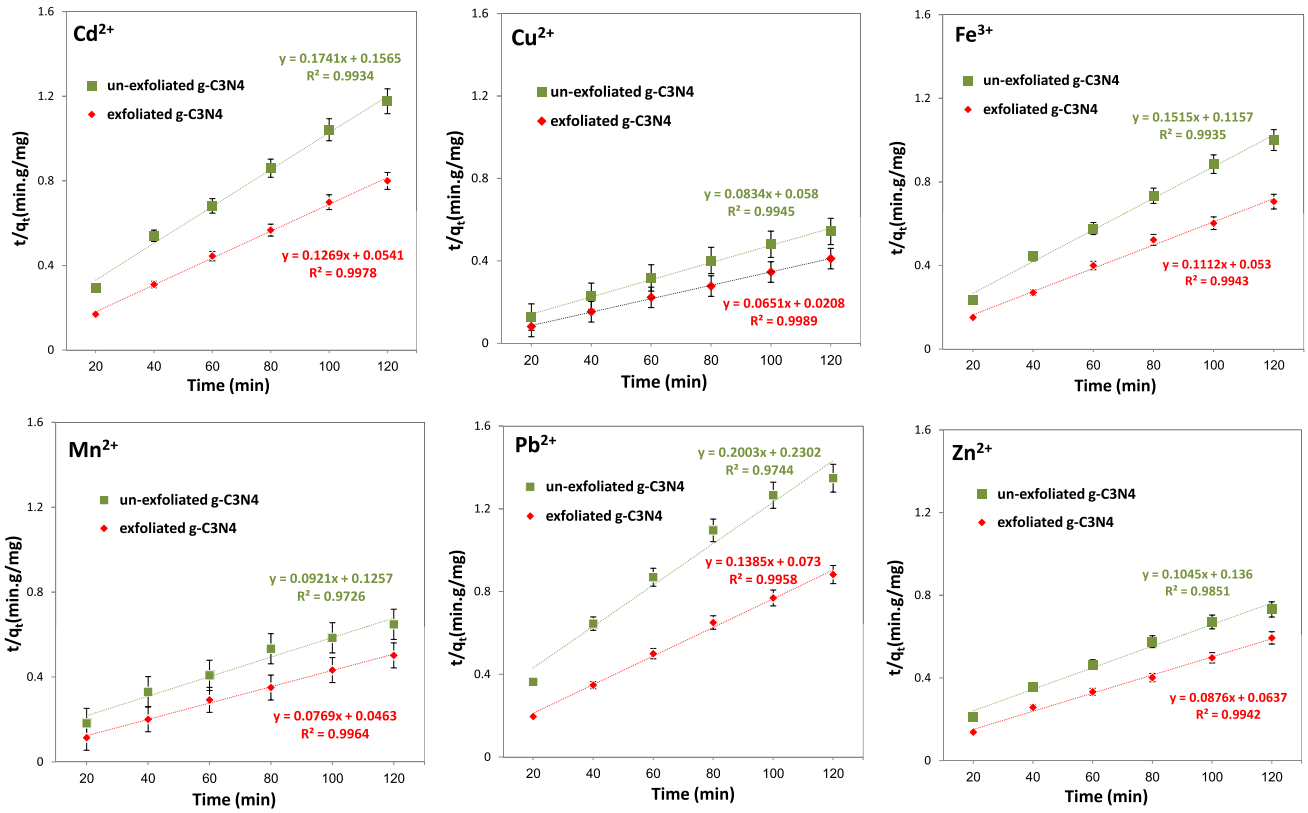

Fig. 5 Pseudo-second-order kinetic plots for ion sorption onto both un-exfoliated and exfoliated g-C_3N_4

experimental data were simulated using the Langmuir and Freundlich isotherm models. The equations used in the Langmuir and Freundlich adsorption isotherm study are defined in Table 2. The sorption data were fit into both the linearized Langmuir and Freundlich models; the results are illustrated in Table 3.

Removal of Toxic Metal Ions from Natural AMD Wastewater

To further investigate how the exfoliated g-C_3N_4 works as an adsorbent, actual AMD wastewater was gathered from the low-grade sulphur deposit at the Sungun copper mine.

Table 2 Mathematical equations applied in adsorption isotherm study of metal ions onto exfoliated g-C_3N_4 nanoadsorbents

Models	Linear Eq.	Plot	Calculated coefficient
Langmuir	$\frac{C_e}{q_e} = \frac{1}{q_m K_L} + \frac{C_e}{q_f}$	$\frac{C_e}{q_e}$ vs C_e	$K_L = \frac{\text{Slope}}{\text{Intercept}}$ $q_m = \text{Slope}^{-1}$
Freundlich	$\log q_e = \log K_F + \frac{\log C_e}{n}$	Log q_e vs log C_e	$K_F = 10^{\text{Intercept}}$ $n = \text{Slope}^{-1}$

C_e is the metal ion concentration (mg/L) at equilibrium; q_e is the amount of metal ions adsorbed per gram of adsorbent at equilibrium (mg/g of adsorbent)

Table 3 Isotherm parameters of Cu^{2+}, Zn^{2+}, and Pb^{2+} adsorption on the exfoliated g-C_3N_4

Metal ion	Langmuir Model			Freundlich model		
	q_m	K_L	R^2	$\frac{1}{n}$	K_F	R^2
Pb^{2+}	88	6.0×10^{-3}	0.970	0.47	3.5	0.902
Cu^{2+}	232	6.3×10^{-3}	0.984	0.44	11.3	0.925
Zn^{2+}	141	1.6×10^{-2}	0.992	0.27	23.9	0.990

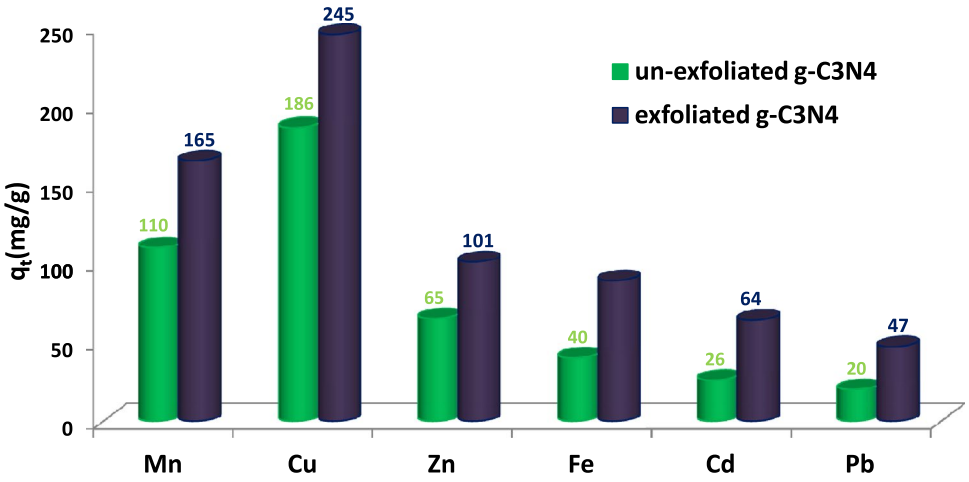

Fig. 6 Comparison of AMD removal between unexfoliated and exfoliated g-C_3N_4 (contact time = 120 min, T = 25 °C)

As seen in Fig. 6, the exfoliated g-C_3N_4 nano-adsorbents efficiently removed the metals.

Reusability and Cost Assessment

Reusability through adsorption/desorption cycles for metal ions is an important factor for long-term sorbent applications. So, the recycling times of g-C_3N_4 for metal ion removals were studied (6–12 cycles). After sorption, desorption was performed via washing the g-C_3N_4 with HCl or HNO_3 solution, it was thoroughly rinsed with water, then dried, and reused. The sorption capacity of the exfoliated g-C_3N_4 decreased slightly for all metal ions after six cycles of regeneration/reuse tests, with increasing reuse. These results indicate that g-C_3N_4 is chemically stable and reusable, and is a promising candidate for cyclic removal of metal ions from aqueous solutions.

The estimated investment and operational costs (including both fixed and variable costs) ranged from 0.04 \$/m^3 of water treated, if the g-C_3N_4 is used 12 times, to 0.08 \$/m^3 if the g-C_3N_4 is used six times. The highest component of the variable costs is raw materials; fixed costs include lab supplies and packaging. These cost estimates are compared with those of other advanced wastewater treatment technologies in Supplemental Table 1.

Conclusions

Un-exfoliated graphitic carbon nitride (g-C_3N_4) was prepared using a simple thermal decomposition approach and subsequently exfoliated by sonication. Both the un-exfoliated and exfoliated g-C_3N_4 was characterized. The sorption behavior of the as-synthesized g-C_3N_4 was investigated for the uptake of metal ions from a prepared aqueous solution and actual samples of mine-related AMD (from the Sungun copper mine). The results indicated that the sorption capacities of the g-C_3N_4 remarkably increased after exfoliation.

Additionally, the findings revealed that the sorbent properties such as high surface area, morphology, and specific functional groups (binding sites) strongly influence removal efficiency. The sorption processes for all of the metal ions followed second-order kinetics, and the sorption isotherms could be simulated well by both the Langmuir and Freundlich adsorption isotherms based on the correlation coefficients (R^2). However, the Langmuir model fits the metal ion sorption isotherms much better than the Freundlich model. Interestingly, the ion removal results from the actual AMD showed that the g-C_3N_4 has great potential as an adsorbent for the pre-concentration of metal ions. Additionally, the sorption mechanisms appear to be mainly attributable to chemical interactions between the metal ions and the g-C_3N_4 surface. Therefore, the inner-sphere surface complexation mechanism satisfactorily explained this fast sorption.

References

Akcil A, Koldas S (2006) Acid mine drainage (AMD): causes, treatment and case studies. J Clean Prod 14:1139–1145

Alslaibi TM, Abustan I, Ahmad MA, Foul AA (2013) Application of response surface methodology (RSM) for optimization of Cu^{2+}, Cd^{2+}, Ni^{2+}, Pb^{2+}, Fe^{2+}, and Zn^{2+}removal from aqueous solution using microwaved olive stone activated carbon. J Chem Technol Biotechnol 88:2141–2151

Cheng Z, Wu Y, Wang N, Yang W, Xu T (2010) Development of a novel hollow fiber cation-exchange membrane from bromomethylated poly (2,6-dimethyl-1,4-phenylene oxide) for removal of heavy-metal ions. Ind Eng Chem Res 49:3079–3087

Fu F, Wang Q (2011) Removal of heavy metal ions from wastewaters: a review. J Environ Manage 92:407–418

Goettmann F, Fischer A, Antonietti M, Thomas A (2006a) Chemical synthesis of mesoporous carbon nitrides using hard templates and their use as a metal-free catalyst for Friedel-Crafts reaction of benzene. Angew Chem Int Ed 45:4467–4471

Goettmann F, Fischer A, Antonietti M, Thomas A (2006b) Metal-free catalysis of sustainable Friedel-Crafts reactions: direct activation of benzene by carbon nitrides to avoid the use of metal chlorides and halogenated compounds. Chem Commun 43:4530–4532

Hong J, Chen C, Bedoya FE, Kelsall GH, O'Hare D, Petit C (2016) Carbon nitride nanosheet/metal–organic framework nanocomposites with synergistic photocatalytic activities. Catal Sci Technol 6:5042–5051

Hu R, Wang X, Dai S, Shao D, Hayat T, Alsaedi A (2015) Application of graphitic carbon nitride for the removal of Pb(II) and aniline from aqueous solutions. Chem Eng J 260:469–477

Huisman JL, Schouten G, Schultz C (2006) Biologically produced sulphide for purification of process streams, effluent treatment and recovery of metals in the metal and mining industry. Hydrometallurgy 83:106–113

Li T, Zhao L, He Y, Cai J, Luo M, Lin J (2013) Synthesis of g-C_3N_4/$SmVO_4$ composite photocatalyst with improved visible light photocatalytic activities in RhB degradation. App Catal B Environ 129:255–263

Li X, Pi Y, Wu L, Xia Q, Wu J, Li Z, Xiao J (2017) Facilitation of the visible light-induced Fenton-like excitation of H2O2 via heterojunction of g-C3N4/NH2-Iron terephthalate metal-organic framework for MB degradation. Appl Catal B Environ 202:653–666

Minamisawa M, Minamisawa H, Yoshida S, Takai N (2004) Adsorption behavior of heavy metals on biomaterials. J Agric Food Chem 52:5606–5611

Motsi T, Rowson NA, Simmons MJH (2009) Adsorption of heavy metals from acid mine drainage by natural zeolite. Int J Miner Process 92:42–48

Ning RY (2002) Arsenic removal by reverse osmosis. Desalination 143:237–241

Rahimi E, Mohaghegh N (2016) Removal of toxic metal ions from Sungun acid rock drainage using mordenite zeolite, graphene nanosheets, and a novel metal–organic framework. Mine Water Environ 35:18–28

Rahimi E, Mohaghegh N (2017) New hybrid nanocomposite of copper terephthalate MOF-graphene oxide: synthesis, characterization and application as adsorbents for toxic metal ion removal from Sungun acid mine drainage. Environ Sci Pollut Res 24:22353–22360

Ren XM, Chen CL, Nagatsu M, Wang XK (2011) Carbon nanotubes as adsorbents in environmental pollution management: a review. Chem Eng J 170:395–410

Shen C, Chen C, Wen T, Zhao Z, Wang X, Xu A (2015) Superior adsorption capacity of g-C_3N_4 for heavy metal ions from solutions. J Colloid Interf Sci 456:7–14

Skousen J, Zipper CE, Rose A, Ziemkiewicz PF, Nairn R, McDonald LM, Kleinmann RL (2017) Review of passive systems for acid mine drainage treatment. Mine Water Environ 36:133–153

Srivastava NK, Majumder CB (2008) Novel biofiltration methods for the treatment of heavy metals from industrial wastewater. J Hazard Mater 151:1–8

Wang Q, Wang XK, Chai ZF, Hu WP (2013) Low-temperature plasma synthesis of carbon nanotubes and graphene based materials and their fuel cell applications. Chem Soc Rev 42:8821–8834

Yan TT, Chen H, Wang X, Jiang F (2013) Adsorption of perfluorooctane sulfonate (PFOS) on mesoporous carbon nitride. RSC Adv 3:22480–22489

Zhao GX, Li JX, Ren XM, Chen CL, Wang XK (2011) Few-layered graphene oxide nanosheets as superior sorbents for heavy metal ion pollution management. Environ Sci Technol 45:10454–10462